



Shahrood University of
Technology



Iranian Society of
Mining Engineering
(IRISME)

Sensitivity Analysis of Tunnel Excavation Damage Zone in Jointed Rock Masses: A DFN-DEM Approach

Mahan Amirkhani¹, Mojtaba Bahaaddini^{1*}, Alireza Kargar¹, and Amin Hekmatnejad²

1. School of Mining Engineering, College of Engineering, University of Tehran, Tehran, Iran

2. Departamento de Ingeniería de Minería, Escuela de Ingeniería, Pontificia Universidad Católica de Chile, Chile

Article Info

Received 7 April 2025

Received in Revised form 10 May 2025

Accepted 2 June 2025

Published online 2 June 2025

DOI: [10.22044/jme.2025.16037.3091](https://doi.org/10.22044/jme.2025.16037.3091)

Keywords

Damage zone

Jointed rock mass

Discrete fracture network

Fracture intensity

Discrete element method

Abstract

The stability of tunnels and underground openings in jointed rock masses is significantly influenced by the development an Excavation Damage Zone (EDZ), where discontinuities alter stress distribution and the fractured propagation zone. In previous studies on EDZ, rock mass is commonly considered as a continuum medium, while the joint system can dictate the size of EDZ. This study aims to investigate the EDZ around a tunnel excavated in a jointed rock mass using the Discrete Fracture Network (DFN) and Discrete Element Method (DEM). Three DFN models with different fracture intensities of 0.5, 1.0, and 1.5 m²/m³ were simulated to explore the progressive failure mechanisms and damage evolution around a tunnel. The DFN models were then imported into the DEM code. The area of the plastic zone was considered a representative measure of the EDZ. The influence of joint mechanical properties, including cohesion, friction angle, normal, and shear stiffnesses, was investigated. A dimensionless sensitivity analysis was conducted to evaluate and compare the influence of each parameter. The results show that the joint friction angle is the most influential parameter in all fracture intensities. These insights provide a more precise understanding of joint behaviour and its impact on tunnel stability in different geological settings.

1. Introduction

The stability of underground excavations in fractured rock masses is a critical concern in rock engineering, particularly for tunnelling projects. The Excavation Damage Zone (EDZ) refers to the region around a tunnel where the rock mass properties have been altered due to stress redistribution, fracturing, and damage by the excavation process. EDZ can significantly influence the long-term performance, and stability of the structure. This zone is characterized by changes in rock permeability, stiffness, and strength, which are induced by excavation methods such as blasting or Tunnel Boring Machines (TBM) [1]. The EDZ can be further divided into High-Damage Zones (HDZ) and Weak-Damage Zones (WDZs), where the HDZ is close to the excavation and experiencing the most significant deterioration [2, 3]. The EDZ is considered to be physically less stable, and can form a continuous and highly

permeable pathway for groundwater flow, which affects tunnel support structure design, construction, and surrounding rock mass stability [4]. The presence of the EDZ around a tunnel perimeter is of significant concern about safety, stability, costs, and overall performance of the tunnel [1].

Understanding the extent and characteristics of EDZ is essential for designing support systems as well as assessing the stability, safety, and performance of tunnels, particularly in challenging geological conditions where the rock mass is highly jointed and discontinuities dominate the mechanical behaviour of the rock mass. The extent and characteristics of the EDZ depend on various factors, including the excavation method, rock properties, and tunnel depth [5].

To understand the factors influencing the EDZ of tunnels, several key aspects need to be



considered based on the previous studies. The impacts of excavation method [6], in-situ stress and stress redistribution aspects [7], rock mass properties [3], geological conditions [8], hydrogeological conditions [9], tunnel geometry and depth [10], construction and management practices [11] are amongst parameters have been studied in previous researches.

Discontinuities such as joints, fractures, faults, and bedding planes play a critical role in the rock mass behaviour during tunnel excavation, impacting the formation and characteristics of the EDZ around underground openings. The presence of pre-existing structural weaknesses features can alter stress distribution, fracture propagation, rock mass degradation, and additional damage, which affect the stability of the surrounding rock masses. These influences lead to variations in EDZ characteristics compared to intact rock conditions. The EDZ in jointed rock masses is often dominated by pre-existing fractures rather than new stress-induced cracks. Persistent fractures also facilitate deeper damage propagation, while non-persistent joints may arrest crack growth [12]. Therefore, exploring the role of discontinuities is essential to understanding the complex characteristics of EDZ.

The evaluation of EDZ has been widely investigated through theoretical, empirical, experimental, and numerical approaches. Wu et al. [13] developed a simplified theoretical method for determining the EDZ based on strain energy density release. Sharan et al. [14], and Zareifard, and Fahimifar [15] derived theoretical closed-form solutions for displacement fields surrounding circular excavations in elastic-brittle-plastic rock masses using the Hoek-Brown failure criterion. Park et al. [16] developed analytical solutions to predict displacements around a circular tunnel based on the Mohr–Coulomb, and Hoek–Brown failure criteria. Roatesi [17] derived a closed-form solution in finite and infinite rock masses based on the unified strength theory in plane strain condition, and analysed the effect of intermediate principal stress, Young's modulus, and dilatation on the stress and displacement fields of EDZs. Huang et al. [18] developed a theoretical model for the damage zone based on the Drucker–Prager criterion, considering the elastic-plastic theory. However, the complex mechanical behaviour of jointed rock mass surrounding underground openings has been simplified in theoretical models. The jointing system has been mainly ignored in these analytical approaches and replaced by homogenized rock materials as well.

The empirical estimation of failure depth around openings was initially estimated by Martin et al. [19], which was later improved by additional case studies of Diederichs [20]. This empirical method has been employed to predict the depth of brittle spalling around tunnels [21, 22]. Yang et al. [23] estimated the rock mass properties of the EDZ using the generalized Hoek-Brown damage criterion and acoustic testing. Fu et al. [24] studied the failure mechanism of circular tunnels reinforced with concrete layers under uniaxial compression through experiments and numerical modelling.

Some efforts have also been undertaken to simulate EDZ using numerical approaches. Golshani et al. [25] simulated the EDZ around a circular opening in a brittle rock mass using an extended microcracking based on a continuum damage model. Yang et al. [26], based on the results of their simulations, found that the development of EDZ around an opening is strongly dependent on the geo-stresses. Perras et al. [27] numerically evaluated the depth of the damaged area and developed equations for the estimation of the EDZ zone of circular tunnels in the brittle rock mass. Ren et al. [28] investigated the plastic damage zone in an elastic–plastic damage FLAC3D numerical method for jointed rock mass. Fan et al. [29] and Feng et al. [30] studied the effect of stress unloading on the EDZ, using theoretical and numerical simulations. Haeri and Sarfarazi [31] developed a multi-laminate-based model to simulate the elasto-plastic and strain-hardening behaviour of rocks. Chen et al. [32] proposed a phase field model to simulate EDZ around tunnels based on non-linear fracture mechanics. Review of the previous numerical studies on EDZ shows that most of these studies have been focused on continuum-based numerical approaches. A limited number of studies have been carried out to simulate EDZ using discontinuous approaches.

As explained above, the stability of the rock mass surrounding excavation openings may be significantly controlled by the presence of discontinuities [33, 34], and recognizing the discontinuous rock medium role is essential [35, 36]. Some numerical efforts have been carried out to highlight the role of discontinuities [37–39], and show that the discontinuities' impact on the EDZ can be more than the strength of intact rocks at the micro-scale [40, 41] and macro-scale [42, 43]. Several key factors regarding the influence of discontinuities on EDZ characteristics needs be considered such as stress redistribution and fracturing mechanisms [42], joint geometry, and

mechanical properties [44, 45], dynamic effects and blasting [46, 47]. Numerical modelling can play a vital role in exploring the complex mechanical characteristics of EDZ in jointed rock masses. The Discrete Element Method (DEM) has been widely adopted to simulate the mechanical behaviour of jointed rock masses due to its explicit ability to model rock blocks' interactions. DEM was first developed [48] for geomechanical applications, demonstrating its effectiveness in capturing discontinuous deformation. Since then, DEM has been widely employed for various rock engineering problems including rock slope stability, underground mining, and tunnelling [49]. DEM models help in understanding the interaction between joint networks and in situ stresses, revealing complex fracturing mechanisms that can compromise tunnel stability [42]. Amongst DEM codes, UDEC and 3DEC have shown promising results in the simulation of the effects of joint geometrical and mechanical properties in the estimation of induced damage zones around underground openings [50, 51]. These codes are suitable numerical tools to study the mechanical behaviour of discontinuous media where discontinuities are simulated explicitly, and their mechanical responses can be understood more realistically. In highly jointed conditions, the efficiency of these codes decreases due to high computational time. However, these codes can provide acceptable and valid results in a jointed rock mass condition.

Discrete Fracture Networks (DFN) are computational or stochastic representations of joints within the rock masses that explicitly model their joint geometry [52]. Unlike continuum approaches, combined DFN-DEM models treat fractures as discrete entities, enabling accurate simulation of discontinuity-controlled failure mechanisms as well as stress redistribution around excavations due to fracture interaction [53]. Some efforts have been undertaken to simulate the damage zone around openings using kinematic stability analyses using DFN models [54]. However, stress distribution around openings has a significant role in the size of the EDZ, as explained earlier. Therefore, analysing the EDZ in tunnels using combined DFN-DEM models can provide a fruitful tool to explore the complex damaging mechanisms around tunnels and underground excavations.

Despite several studies on the extent of the EDZ and effective parameters, a systematic quantification and comparison of the effects of discontinuities on the plastic damage zone cannot

be found in the literature. Most of the previous studies are restricted to the assumptions of continuum media and a uniform damage zone, without considering the effect of the fracture joint system on the extent of the EDZ. Therefore, the behaviour of EDZ in discontinuous rock masses remains poorly understood. A systematic evaluation of the EDZ, where the rock mass medium has been considered discontinuous and joints' geometrical and mechanical properties have been simulated explicitly, can improve our understanding of the EDZ.

This paper aims to investigate the effect of joint mechanical and geometrical properties on EDZ using combined DFN-DEM models. Models with different fracture intensities were generated using the DFN technique, and the generated models were imported into DEM models. Through a comprehensive sensitivity analysis, the influence of joint mechanical properties, including joint normal and shear stiffnesses, cohesion and friction angle, on the EDZ at different joint fracture intensities were investigated.

2. Theory and Background

In this section, an overview of the theoretical framework of the numerical methods and the approach to dimensionless sensitivity analysis is presented.

2.1. Fundamental principles of DEM

The Discrete Element Method (DEM) is a numerical approach that facilitates finite displacements and rotations of discrete bodies including complete detachment, while automatically detecting new contacts as computations progress [55]. DEM was developed by Cundall in the early 1970s to analyse discontinuous rock masses [48]. This method partitions the rock mass into discrete blocks, which are connected through predefined contacts. These contacts serve as pathways for crack propagation and are defined as the boundaries of the model. Additionally, the displacements and forces at the contacts are computed during the analysis [56, 57].

In DEM, joints are represented as the separating surfaces between the edges of adjacent blocks. These joints act as surface elements that enable adjacent block edges to interact through impact, relative sliding, or separation and closure. The contacts are characterized by finite stiffness in both the normal and shear directions, modelled using normal and shear springs, as shown in Figure 1. Consequently, the force exerted on each spring is

computed based on its displacement, as described below:

$$\Delta F_n = k_n \Delta u_n \quad (1)$$

$$\Delta F_s = k_s \Delta u_s \quad (2)$$

where ΔF , Δu , and k are the force, displacement, and stiffness coefficients, respectively, and the n and s subscripts denote the normal and shear directions, respectively. Additionally, the shear stress on joint surfaces is constrained by cohesion (c), friction angle (φ), and the normal stress acting on the joint surfaces (σ_n), as defined by the Mohr-Coulomb failure criterion, as follows:

$$|\tau| \leq c + \sigma_n \tan \varphi \quad (3)$$

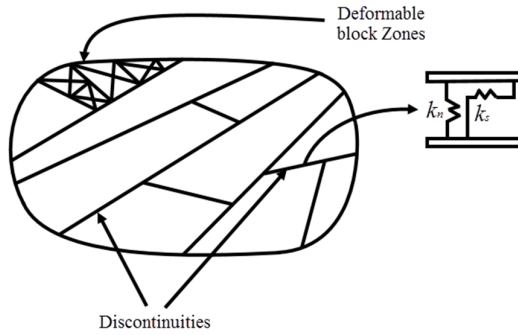


Figure 1. Rigid and deformable blocks and the simulation of characterization of joints using springs [56]

UDEC is based on the Distinct Element Method (DEM), in which a discontinuous rock mass is simulated as an assembly of discrete, rigid or deformable blocks. The mechanical interaction between adjacent blocks is governed by force-displacement laws at contacts, characterized by normal and shear stiffness, cohesion, and frictional resistance. Block separation, sliding, and rotation are explicitly allowed, enabling the simulation of complex deformation and failure mechanisms. This numerical framework allows UDEC to accurately capture the non-linear mechanical behaviour of jointed rock masses under various loading and excavation conditions.

2.2. EDZ estimation via Mohr-Coulomb criterion

Continuous methods, such as the phase-field approach, have been employed in previous studies to quantify the EDZ [32]. In this study, the extent of the EDZ was evaluated based on the development of plastic zones, using the Mohr-

Coulomb failure criterion implemented in UDEC. According to this model, yielding occurs when the major and minor principal stresses at an element satisfy the Mohr-Coulomb condition, resulting in plastic deformation. The stress state can be classified into three main categories:

- Stable condition: The Mohr's circle lies entirely within the failure envelope, indicating that the element remains in the elastic regime with no sign of yielding.
- Critical (limit equilibrium) condition: The Mohr's circle is tangent to the failure envelope, suggesting that the element is at the onset of yielding and is about to enter the plastic zone.
- Unstable condition: Mohr's circle intersects the failure envelope, meaning the element has yielded and exhibits plastic behaviour.

The failure envelope is defined by the Mohr-Coulomb yield function, as follows [58]:

$$f^s = \sigma_1 - \sigma_3 N_\varphi + 2c\sqrt{N_\varphi} \quad (4)$$

and a tension yield function is obtained from [58]:

$$f^t = \sigma_t - \sigma_3 \quad (5)$$

where σ_1 and σ_3 are the major and minor principal stresses, respectively, and N_φ is [58]:

$$N_\varphi = \frac{1 + \sin(\varphi)}{1 - \sin(\varphi)} \quad (6)$$

The negative, zero, and positive values of each yield function indicate the stable, critical, and unstable (plastic behaviour) of the studied triangular mesh zones, respectively. A FISH function was developed to compute the total area of these yielded zones, which was subsequently used as a quantitative measure for the EDZ. This approach ensures consistency with the constitutive framework of UDEC and provides an objective basis for comparing the influence of joint parameters on damage evolution.

2.3. Dimensionless sensitivity analysis

Sensitivity analysis is a method used to evaluate the stability of a system [59]. A character P is considered dependent on n factors ($P=f\{\alpha_1, \alpha_2, \dots, \alpha_n\}$) within the system. During the sensitivity analysis process, one of these factors (α_k) is varied within a specified range while monitoring the resulting changes in the system's parameter (P). The analysis begins by varying the factor (α_k) within its range while keeping all other factors

constant, subsequently establishing a relationship between the system's parameter (P) and α_k , as expressed below [59]:

$$P = f(\alpha_1^*, \dots, \alpha_{k-1}^*, \alpha_k, \alpha_{k+1}^*, \dots, \alpha_n^*) = \varphi(\alpha_k^*) \quad (7)$$

where “*” superscript means the constant (basic) values of the factors. The P- α_k diagram obtained from Equation (7) and its slope illustrate the sensitivity of P to variations in α_k (Figure 2). It is evident that a change in α_k near α_{k1} results in a more significant variation in P compared to a change in α_k near α_{k2} .

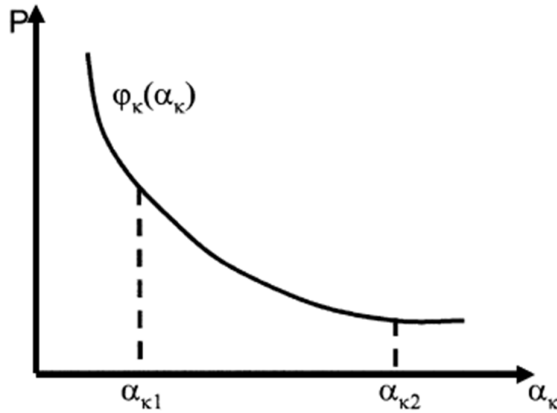


Figure 2. Schematic curve of the relationship between P and α_k [59]

The sensitivity analysis described above is effective for evaluating the impact of a single factor on the system. However, the system is influenced by multiple factors that affect the parameter P in different ways, making it difficult to compare their sensitivities using this method. To address this challenge, a dimensionless sensitivity analysis is proposed.

In dimensionless sensitivity analysis, a dimensionless function known as the “sensitivity function” is defined as the ratio of the relative error of the parameter $\delta P = |\Delta P|/P$ to the relative error of the factor $\delta \alpha_k = |\Delta \alpha_k|/\alpha_k$ [59]:

$$S_k(\alpha_k) \triangleq \left(\frac{|\Delta P|}{P} \right) / \left(\frac{|\Delta \alpha_k|}{\alpha_k} \right) = \left| \frac{\Delta P}{\Delta \alpha_k} \right| \frac{\alpha_k}{P} \quad (8)$$

$k = 1, 2, \dots, n$

As the magnitude of $\Delta \alpha_k / \alpha_k$ decreases and approaches zero, the sensitivity function $S_k(\alpha_k)$ converges to Equation 9, by substituting $P = \varphi(\alpha_k)$ from Equation (7) **Error! Reference source not found.** into Equation (8):

$$S_k(\alpha_k) = \left| \frac{d\varphi_k(\alpha_k)}{d\alpha_k} \right| \frac{\alpha_k}{P} \quad k = 1, 2, \dots, n \quad (9)$$

Finally, the dimensionless sensitivity factor S_k^* of α_k is obtained by substituting $\alpha_k = \alpha_k^*$ (i.e. the base value of α_k) into Equation 10, as shown in Equation 10, The dimensionless sensitivity factor of each parameter indicates the sensitivity of the system's behavior to that parameter. The impact of error in each factor increases with the increase in its sensitivity factor [59].

$$S_k^* = S_k(\alpha_k^*) = \left(\frac{d\varphi_k(\alpha_k)}{d\alpha_k} \right) \alpha_k = \alpha_k^* \frac{\alpha_k^*}{P^*} \quad (10)$$

$k = 1, 2, \dots, n$

In this study, the sensitivity analysis outlined above was applied to investigate the impact of joint mechanical properties on the EDZ.

3. Methodology

3.1. Generation of Discrete Fracture Network (DFN) models

In this study, the rock mass is considered as a discontinuous medium and consists of intact rock blocks and fractures. These fractures were simulated using the DFN model. In this study, the classical Baecher approach was used for DFN modelling. Firstly, a cubic block with an edge length of 40 meters was considered, and then fractures were simulated by circular discs. These circular discs were distributed using the Poisson distribution, and their lengths were assumed to be normally distributed. The average radius of fractures was assigned 10 m with a standard deviation of 1 m.

Investigating the impact of fracture intensity is one of the most important concerns of this study. To this end, the fracture intensity parameter of P_{32} (total area of fractures in the unit of volume) was considered as the criterion for jointing severity. Three DFN patterns with P_{32} values of 0.5, 1.0 and 1.5 m^2/m^3 been were generated and then a 2D section for each model was prepared and imported to the numerical model.

3.2. Numerical simulation

The El Teniente mine in Chile is the largest underground copper deposit in the world [60]. This study investigates a vertical section of a horizontal tunnel in this mine, and this tunnel has an orientation of N95°E. The tunnel has a horseshoe cross-section, as shown in Figure 3. In the

numerical models, the tunnel was simulated at the center of the $40\text{ m} \times 40\text{ m}$ square boundary. As noted earlier, the fracture network was simulated using the DFN model, where the primary DFN models were generated in three dimensions by circular discs using the classical Baecher approach [61], and then 2D sections from these models were considered for numerical analyses in universal

distinct element code (UDEC). The model dimension was set 10 times the tunnel width to minimize boundary effects (Figure 3). There jointing conditions of slightly fractured ($P_{32}=0.5\text{ m}^2/\text{m}^3$), moderate fractured ($P_{32}=1.0\text{ m}^2/\text{m}^3$) and highly fractured ($P_{32}=1.5\text{ m}^2/\text{m}^3$) were considered, as shown in Figure 4.

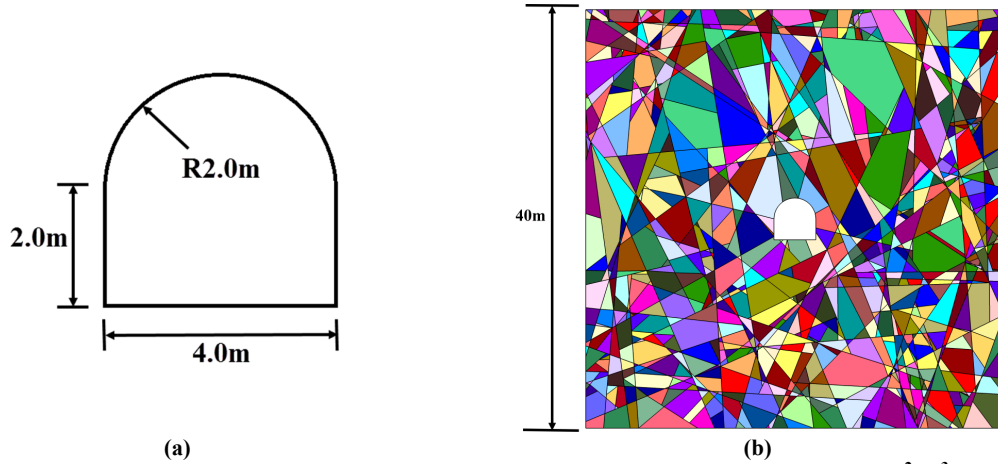


Figure 3. a) The geometry of tunnel and b) A typical generated DFN model ($P_{32} = 1.0\text{ m}^2/\text{m}^3$)

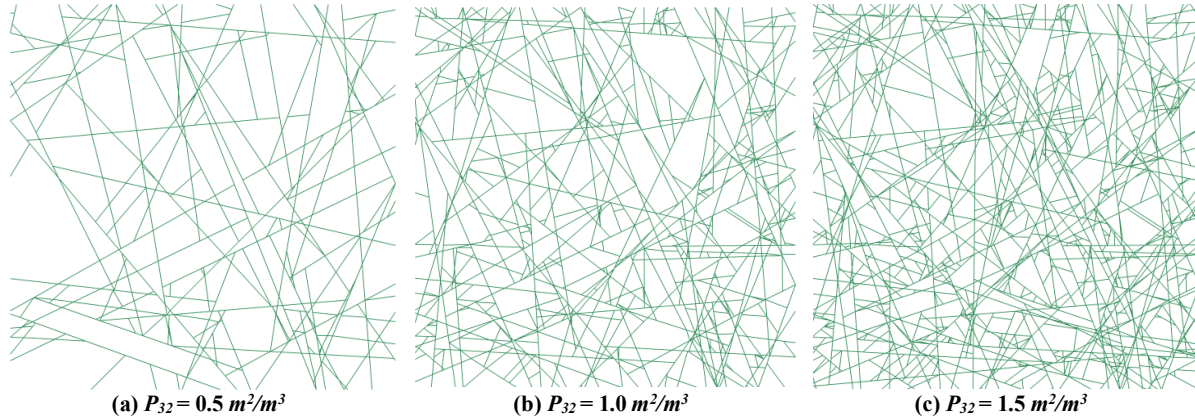


Figure 4. DFN patterns for different fracture intensities

The rock mass was considered discontinuous, and the intact rock was assumed isotropic. The vertical cross-section of the tunnel is subjected to major and minor vertical principal stresses, as well as a horizontal stress component, with values of $\sigma_1=53.59\text{ MPa}$, $\sigma_2=50.45\text{ MPa}$, and $\sigma_3=30.77\text{ MPa}$, respectively. However, σ_2 is the out-of-plane component, while σ_1 is inclined at an angle of 2.11 degrees clockwise relative to the horizontal axis. The lower boundary condition of the model was fixed, and the in-plane horizontal principal stress of 53.59 MPa was applied to the left and right boundaries of the model. However, the vertical stress of 30.77 MPa was applied to the upper horizontal boundary, based on the in-situ stress

condition. The intact rock was considered deformable and linear elastic, with the Mohr-Coulomb failure criterion. The Mohr-Coulomb failure criterion has been commonly employed in geomechanical modeling, likely due to its computational efficiency in numerical codes and the widespread availability of its input parameters (cohesion and friction angle) in previous studies [62]. The mechanical properties of the intact material are summarized in Table 1. It should be noted that the validity of the model was first evaluated using the Kirsch models for a circular tunnel. Then, based on the tunnel dimension of El Teniente mine and fracture intensities, the numerical models were created. The plot of

displacement magnitude for $P_{32}=1.0 \text{ m}^2/\text{m}^3$ is shown in Figure 5. Finally, the extent of the plastic zone was measured using a fish function after reaching the static equilibrium condition, and the value of the plastic zone extent was considered as EDZ.

Table 1. Mechanical properties of the intact rock

Properties	Values
Density (kN/m^3)	28
Young modulus (GPa)	55
Poisson's ratio	0.25
Internal friction angle (Deg.)	43
Cohesion (MPa)	25
Peak tensile strength (MPa)	13
Residual tensile strength (MPa)	13

3.2. Sensitivity analysis

In this study, the effect of four parameters of joint normal stiffness (k_n), joint shear stiffness (k_s), joint friction angle (φ), and joint cohesion (C) on the EDZ was investigated. The extent of the plastic zone around the tunnel can lead to breakouts,

collapses, and rock bursts. Therefore, the extent of the plastic zone around the tunnel was used as the criterion for tunnel EDZ. Each of these factors was varied within the specified range noted in Table 2, and the effect of these variations on the area of the plastic zone was investigated.

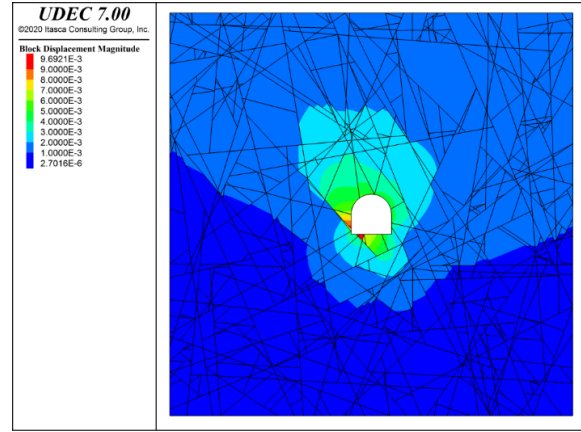


Figure 5. Displacements of the basic moderate fractured model ($P_{32}=1.0\text{m}^2/\text{m}^3$)

Table 2. The studied parameters, their basic values, and their possible ranges

Parameter name	Basic value	Variation range
Normal stiffness (GPa/m)	114	100-350
Shear stiffness (GPa/m)	38	10-110
Joint friction angle (Deg.)	40	10-40
Joint cohesion (kPa)	38	20-120

4. Results and Discussion

The basic numerical model with the parameters shown in Table 2 was first constructed. Then, by keeping all other parameters constant and varying one parameter within the specified range, the changes in EDZ extent are investigated by measuring the plastic zone extent (Figure 6). Subsequently, correlation functions between each parameter and EDZ extent was developed, and the corresponding sensitivity functions were determined. Finally, a dimensionless sensitivity factor was derived for each parameter from its sensitivity function.

4.1. Parametric study of joint mechanical properties

Based on the undertaken numerical analyses for each fracture intensity, the correlation between joint normal stiffness, shear stiffness, friction angle, and cohesion with EDZ was determined, and the results are presented in Figures 7 to 9. The results show that the increase in joint normal stiffness results in a decrease in the size of EDZ. The joint normal stiffness at block interfaces

controls normal deformation and overlap between blocks and decreases the deformation characteristics of blocks at the tunnel boundary. Therefore, the increase in joint normal stiffness leads to a decrease in the extent of the plastic (damage) zone around the tunnel.

The shear behavior of rock joints before failure is predominantly controlled by the shear stiffness of the joint surfaces, while the joint friction angle governs the shear response both before and after the onset of shear failure. This is attributed to the fact that the joint peak and residual friction angles are identical across all models. The reduction in joint shear stiffness leads to the formation of more fractures at the specified stress condition. These early fractures weaken the joint system. As loading continues, more blocks experience stress concentrations caused by their rotations, and thereafter, the extent of damage is increased. However, the shear slip on joint surfaces is controlled by the joint friction angle. The EDZ is more significantly controlled by the joint friction angle, and the increase in joint friction angle can considerably suppress block movements and the corresponding reduction in the damage zone. The

increase in cohesion of joint surfaces resulted in a decrease in EDZ size. However, a specific statistically significant equation was not found in the studied range of 20 to 120 kPa for fracture intensities of 0.5 to 1.5 m²/m³.

Both cohesion and friction angle along joint surfaces play a fundamental role in preventing slip between adjacent rock blocks. Slip along discontinuities promotes both translational and rotational movements, which in turn elevate the shear and compressive stresses acting on the blocks. A reduction in cohesion or friction facilitates such displacements, leading to a higher

number of blocks and triangular mesh elements exceeding their yield thresholds. As a result, lower cohesion values contribute to a greater extent of the excavation damaged zone (EDZ), whereas higher cohesion suppresses plastic deformation. This inverse relationship between these two factors and EDZ size is clearly illustrated in Figures 7 to 9. Accordingly, a decreasing trend in EDZ extent is observed across all three levels of fracture intensity. However, the data of cohesion do not exhibit a strong correlation that would allow for an accurate regression fit.

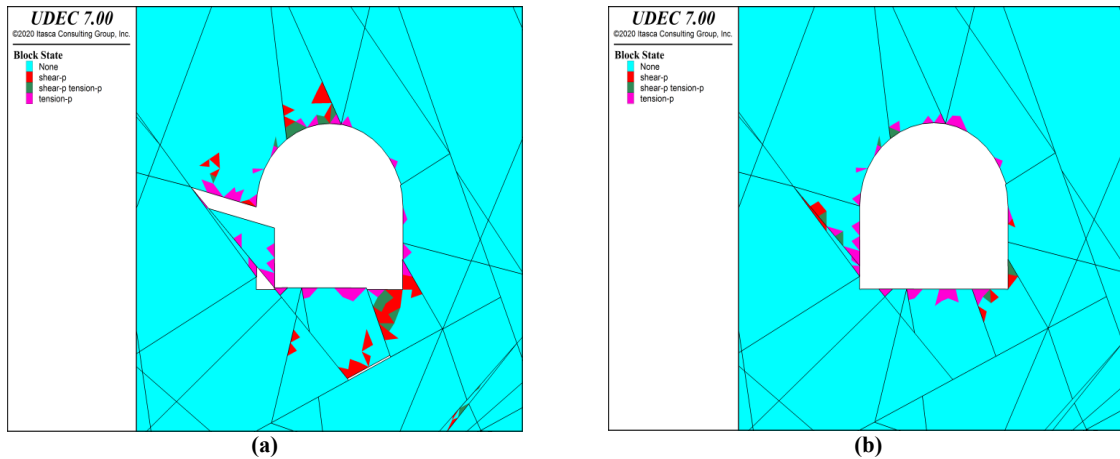


Figure 6. Plastic zone around the models for $P_{32} = 1.0\text{m}^2/\text{m}^3$ indicated by the Mohr Coulomb failures criterion for a) $\phi = 10^\circ$ and b) $\phi = 30^\circ$

4.2. Dimensionless sensitivity analysis of parameters

Direct interpretation of Figures 7 to 9 does not provide a definitive assessment of parameter sensitivity, primarily due to the differing units and variation ranges among the input variables. To enable a meaningful sensitivity analysis, it is essential to establish a functional relationship between each input parameter (e.g. normal stiffness) and the system response (EDZ extent). Among several candidate regression models, the fitted curves presented in Figures 7 to 9 were selected based on their ability to closely replicate the numerical results. These regression equations serve as the basis for quantifying the relative influence of each factor on the behavior of the rock mass around the tunnel. As explained earlier, dimensionless sensitivity indices are required for a consistent comparison of parameter effects. In this study, the sensitivity factors for each parameter were determined using the methodology described in Section 2.3, and the results are summarized in Table 3. These dimensionless indices enable a direct comparison of the influence of parameters

with differing physical units and scales. Based on the dimensionless factors summarized in Table 3 and comparing the impact of each factor on the damage area, it can be concluded that the joint friction angle is the most effective parameter on the EDZ in all fracture intensities. It is interesting to note that the impact of joint friction angle is considerably higher in moderately fractured rocks, compared to slightly and highly fractured rock masses, which is due to the joint system network of DFN. The friction angle of joint surfaces is the most important factor in EDZ extent in all three fracture intensities of P_{32} . The sensitivity analysis factors show that the role of joint friction angle in moderately fractured rock is approximately 11 and 28 times greater than that of shear stiffness and normal stiffness, respectively.

The normal stiffness of joint surfaces is the least effective factor in EDZ extent in the fracture intensities of P_{32} . As this parameter controls the normal deformability of rock blocks at joint interfaces, the increase in normal stiffness results in a decrease in normal overlap between blocks, less deformation of the tunnel, and the

corresponding decrease in extent of EDZ. However, this parameter can only slightly alter the EDZ zone compared to shear strength parameters

due to the significant role of shear stresses at block interfaces in generating the EDZ of jointed rock masses.

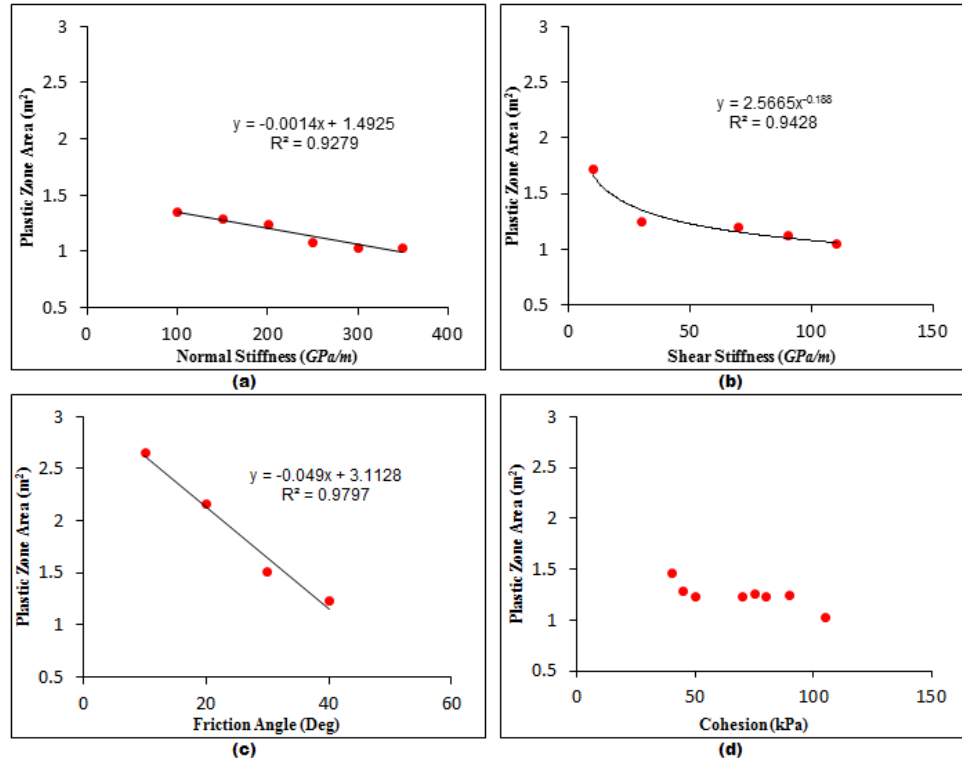


Figure 7. Sensitivity analysis on the effect of joint mechanical properties on the extent of EDZ for $P_{32}=0.5\text{m}^2/\text{m}^3$: a) Effect of joint normal stiffness, b) Effect of joint shear stiffness, c) Effect of joint friction angle, d) Effect of joint cohesion

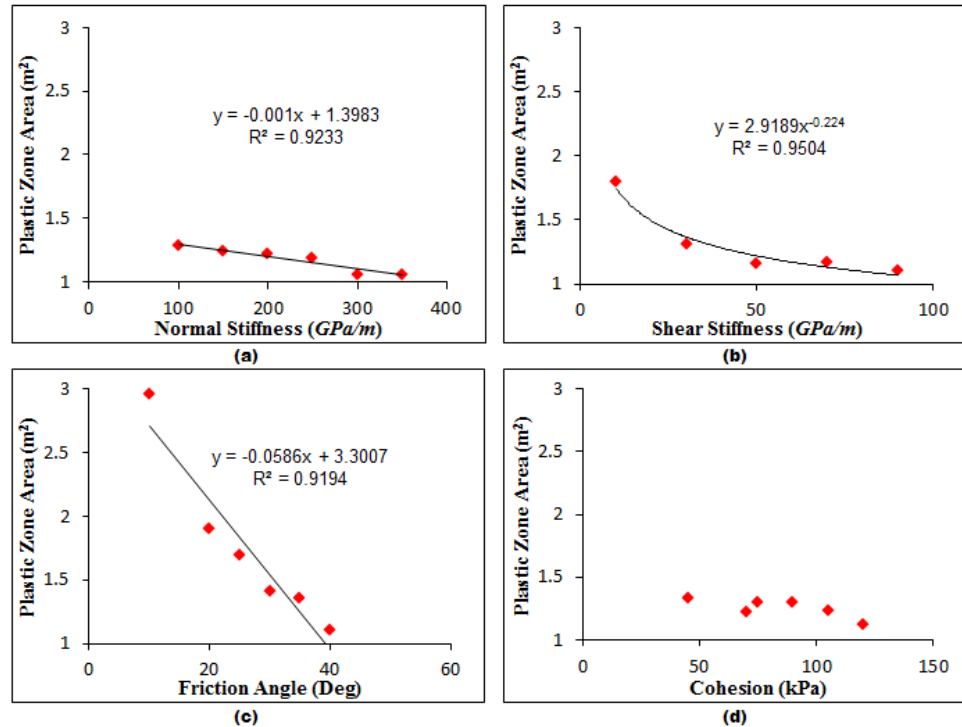


Figure 8. Sensitivity analysis of the effect of joint mechanical properties on the extent of EDZ for $P_{32}=1.0\text{m}^2/\text{m}^3$: a) Effect of joint normal stiffness, b) Effect of joint shear stiffness, c) Effect of joint friction angle, d) Effect of joint cohesion

Table 3. Sensitivity factors for three DFN models

	$P_{32}=0.5$	$P_{32}=1.0$	$P_{32}=1.5$
$S_{k_n}^*$	0.1197	0.0888	0.0940
$S_{k_s}^*$	0.1880	0.2240	0.2290
S_{φ}^*	1.7002	2.4501	1.4377
S_c^*	-	-	-

5. Conclusions

Estimation of the Excavation Damage Zone (EDZ) is of critical importance in underground space and tunneling projects. In this study, the effect of joint mechanical and geometrical properties on the EDZ was investigated using combined DFN-DEM numerical models. Three DFN models having fracture intensities P_{32} of 0.5, 1.0, and $1.5 \text{ m}^2/\text{m}^3$ were generated, and 2D sections were imported into UDEC. Sensitivity analyses on the effect of joint normal stiffness, shear stiffness, friction angle, and cohesion were conducted to evaluate the impact of these parameters on the EDZ around a tunnel in jointed rock masses. The extent of the plastic zone was considered as the EDZ criterion. In this study, the EDZ was quantified by identifying all triangular mesh elements within the intact rock that exhibited plastic yielding under either shear or tensile conditions, as governed by the Mohr-Coulomb failure criterion. The cumulative area of these yielded elements was calculated and considered as a representative measure of the EDZ extent. The analysis quantified the EDZ extent predictions based on variations in joint surface parameters. The results indicate that the joint friction is the most influential parameter on EDZ extent. The influence of the joint friction angle on the extent of the EDZ was considerably greater than other factors in all fracture intensities. The increase in joint cohesion resulted in a decrease in EDZ size, but no statistically significant correlation was found in the studied range of 20–120 kPa. The influence of joint shear stiffness on EDZ extent was found to be significant a decrease was found in EDZ with an increase in joint shear stiffness. The increase in joint normal stiffness also showed a slight decreasing trend in EDZ extent at all fracture intensities due to its effect on normal deformability of blocks at joint interfaces.

6. References

- [1]. Yang, J., Lu, W., Hu, Y., et al. (2015). Numerical simulation of rock mass damage evolution during deep-buried tunnel excavation by drill and blast. *Rock Mechanics and Rock Engineering*. 48: 2045–2059.
- [2]. Dai, J., Gong, F. & Xu, L. (2024). Rockburst criterion and evaluation method for potential rockburst pit depth considering excavation damage effect. *Journal of Rock Mechanics and Geotechnical Engineering*.; 16 (5): 1649–1666.
- [3]. Dai, J., Gong, F., Xu, L., et al. (2023). Weakening laws of rock mass parameters in the excavation damage zone of deep rock tunnels. I In: Wang, S., Huang, R., Azzam, R., Marinos, V.P. (eds) *Engineering Geology for a Habitable Earth: IAEG XIV Congress 2023 Proceedings*, Chengdu, China. IAEG 2023., 517–531.
- [4]. Zhou, J.W., Yang, X.G., Li, H.T., et al. (2011). Analysis of excavation damaged zone of auxiliary tunnel based on field wave velocity test at the Jinping hydropower station. In: *Rock Mechanics: Achievements and Ambitions - Proceedings of the 2nd ISRM International Young Scholars' Symposium on Rock Mechanics*. State Key Laboratory of Hydraulics and Mountain River Engineering, Sichuan University, Chengdu, China, 65–71.
- [5]. Hekmatnejad, A., Crespin, B., Opazo, A., et al. (2020). Investigating the impact of the estimation error of fracture intensity (P_{32}) on the evaluation of in-situ rock fragmentation and potential of blocks forming around tunnels. *Tunnelling and Underground Space Technology*. 106: 103596.
- [6]. Yan, P., Lu, W., Chen, M., et al. (2011). In-situ test research on influence of excavation method on induced damage zone in deep tunnel. *Yanshilixue Yu Gongcheng Xuebao/Chinese Journal of Rock Mechanics and Engineering*. 30 (6): 1097–1106.
- [7]. Yang, D., Li, H-B., Xia, X., et al. (2014). Study of blasting-induced dynamic damage of tunnel surrounding rocks under high in-situ stress. *Yantu Lixue/Rock and Soil Mechanics*. 35 (4): 1110–1122.
- [8]. Pai, L., Pang, W., Wu, H., et al. (2020). Research on the influence of hard-soft interlayer thick structure on tunnel surrounding rock excavation damage. *Journal of Railway Engineering Society*. 37 (1): 73–79.
- [9]. Yuan, D. & Xiao, K. (2025). Water intrush mechanism and the minimum safety thickness of the rock wall of a tunnel crossing a fault fracture zone. *Journal of Geomechanics*. 31 (1): 80–90.
- [10]. Zhang, R., Xie, H.P., Ren, L., et al. (2022). Excavation-induced structural deterioration of rock masses at different depths. *Archives of Civil and Mechanical Engineering*. 22 (2): 81.
- [11]. Huang, L. & Huang, X. (2015) Risk assessment in tunnel portal based on fuzzy AHP comprehensive evaluation. In: *Proceedings - 2015 International*

Conference on Intelligent Transportation, Big Data and Smart City, ICITBS 2015. Wuhan, China. 692–696.

[12]. Bahaaddini, M., Sharrock, G. & Hebblewhite, B.K. (2011). A comparison of physical and numerical experiments on artificial jointed rock masses using PFC3D. *Proc. 2nd International FLAC/DEM Symposium*, Melbourne, Australia: Itasca, 321–330.

[13]. Wu, F., Liu, J., Liu, T., et al. (2009). A method for assessment of excavation damaged zone (EDZ) of a rock mass and its application to a dam foundation case. *Engineering Geology*. 104 (3-4): 254–262.

[14]. Sharan, S.K. (2003). Elastic-brittle-plastic analysis of circular openings in Hoek-Brown media. *International Journal of Rock Mechanics and Mining Sciences*; 40 (6): 817–824.

[15]. Zareifard, M.R., & Fahimifar, A. (2016). Analytical solutions for the stresses and deformations of deep tunnels in an elastic-brittle-plastic rock mass considering the damaged zone. *Tunnelling and Underground Space Technology* 58: 186–196.

[16]. Park, K.H. & Kim, Y. J. (2006). Analytical solution for a circular opening in an elastic-brittle-plastic rock. *International Journal of Rock Mechanics and Mining Sciences*; 43 (4): 616–622.

[17]. Roateşi, S. (2014). Analytical and numerical approach for tunnel face advance in a viscoplastic rock mass. *International Journal of Rock Mechanics and Mining Sciences*. 70: 123–132.

[18]. Huang, F., Zhu, H.H., Li, Q.S., et al. (2016). Field detection and theoretic analysis of loose circle of rock mass surrounding tunnel. *Rock and Soil Mechanics*. 37: 145–150.

[19]. Martin, C.D. & Chandler N.A. (1994). The progressive fracture of Lac du Bonnet granite. *International journal of rock mechanics and mining sciences & geomechanics abstracts*. 31 (6): 643–659.

[20]. Diederichs, M.S. (2007). The 2003 Canadian Geotechnical Colloquium: Mechanistic interpretation and practical application of damage and spalling prediction criteria for deep tunnelling. *Canadian Geotechnical Journal*. 44 (9): 1082–1116.

[21]. Martin, C.D. & Christiansson, R. (2009). Estimating the potential for spalling around a deep nuclear waste repository in crystalline rock. *International Journal of Rock Mechanics and Mining Sciences*. 46 (2): 219–228.

[22]. Perras, M.A., Wannenmacher, H. & Diederichs, M.S. (2015). Underground excavation behaviour of the Queenston formation: tunnel back analysis for application to shaft damage dimension prediction. *Rock Mechanics and Rock Engineering*. 48: 1647–1671.

[23]. Yang, J., Dai, J., Yao, C., et al. (2020). Estimation of rock mass properties in excavation damage zones of rock slopes based on the Hoek-Brown criterion and acoustic testing. *International Journal of Rock Mechanics and Mining Sciences*. 126: 104192.

[24]. Fu, J., Haeri, H., Sarfarazi, V., et al. (2023). Failure

mechanism of circular tunnel supported by concrete layers under uniaxial compression: Numerical simulation and experimental test. *Theoretical and Applied Fracture Mechanics*. 125: 103839.

[25]. Golshani, A., Oda, M., Okui, Y., et al. (2007). Numerical simulation of the excavation damaged zone around an opening in brittle rock. *International Journal of Rock Mechanics and Mining Sciences*. 44 (6): 835–845.

[26]. Yang, H.Q., Zeng, Y.Y., Lan, Y.F., et al. (2014). Analysis of the excavation damaged zone around a tunnel accounting for geostress and unloading. *International Journal of Rock Mechanics and Mining Sciences*. 69: 59–66.

[27]. Perras, M.A. & Diederichs, M.S. (2016). Predicting excavation damage zone depths in brittle rocks. *Journal of Rock Mechanics and Geotechnical Engineering*. 8 (1): 60–74.

[28]. Ren, M., Zhang, Q., Liu, C., et al. (2019). The elastic–plastic damage analysis of underground research laboratory excavation for disposal of high level radioactive waste. *Geotechnical and Geological Engineering*. 37: 1793–1811.

[29]. Fan, Y., Zheng, J.W., Cui, X.Z., et al. (2021). Damage zones induced by in situ stress unloading during excavation of diversion tunnels for the Jinping II hydropower project. *Bulletin of Engineering Geology and the Environment*. 80: 4689–4715.

[30]. Feng, G.L., Chen, B.R., Xiao, Y.X., et al. (2022). Microseismic characteristics of rockburst development in deep TBM tunnels with alternating soft–hard strata and application to rockburst warning: A case study of the Neelum–Jhelum hydropower project. *Tunnelling and Underground Space Technology*. 122: 104398.

[31]. Haeri, H. & Sarfarazi, V. (2016). The deformable multilaminate for predicting the Elasto-Plastic behavior of rocks. *Computers and Concrete, an International Journal*. 18 (2): 201–214.

[32]. Chen, X., Liu, J., Wang, X., et al. (2025). Phase field model of tunnel excavation damage zone. *Computational Particle Mechanics*. <https://doi.org/10.1007/s40571-025-00908-1>.

[33]. Hudson, J.A. (1992). *Rock engineering system. Theory and practice*. Ellis Horwood Series in Civil Engineering: Geotechnics.

[34]. Cai, J.G., Zhao, J. & Hudson, J.A. (1998). Computerization of rock engineering systems using neural networks with an expert system. *Rock Mechanics and Rock Engineering*. 31 (3): 135–152.

[35]. Barton, N. (1973). Review of a new shear-strength criterion for rock joints. *Engineering geology*. 7 (4): 287–332.

[36]. Barton, N.R. (1986). Deformation phenomena in jointed rock. *Geotechnique*. 36 (2): 147–167.

[37]. Brown, E.T. (1987). *Analytical and computational methods in engineering rock*. HarperCollins Publishers Ltd.

[38]. Goodman, R.E., Heuz, F.E., Bureau, G.J. (1972). On modelling techniques for the study of tunnels in jointed

- rock. In: *The 14th U.S. Symposium on Rock Mechanics (USRMS)*, University Park, Pennsylvania, June 1972, ARMA-72-0441.
- [39]. Goodman, R.E. (1976). *Methods of geological engineering in discontinuous rocks*. West Pub Group.
- [40]. Mahabadi, O.K. (2012). *Investigating the influence of micro-scale heterogeneity and microstructure on the failure and mechanical behaviour of geomaterials*. PhD thesis, University of Toronto, Canada.
- [41]. Abdelaziz, A., Zhao, Q., Grasselli, G. (2018). Grain based modelling of rocks using the combined finite-discrete element method. *Computers and Geotechnics*. 103: 73–81.
- [42]. Vazaios, I., Vlachopoulos, N. & Diederichs, M.S. (2019). Assessing fracturing mechanisms and evolution of excavation damaged zone of tunnels in interlocked rock masses at high stresses using a finite-discrete element approach. *Journal of Rock Mechanics and Geotechnical Engineering*. 11 (4): 701–722.
- [43]. Han, G., Zhang, C.C., Zhou, H., et al. (2021) A new predictive method for the shear strength of interlayer shear weakness zone at field scales. *Engineering Geology*. 295: 106449.
- [44]. Wang, C., Liu, X., Yao, W., et al. (2024). Study on rock stability and structural response of shield-driven twin tunnels crossing fault fracture zone based on 3d numerical simulation. *Bulletin of Engineering Geology and the Environment*; 83 (7): 106449.
- [45]. Chen, S. & Zhu, Z. (2022). Numerical study on tunnel damage subject to blast loads in jointed rock masses. *Environmental Earth Sciences*; 81 (24): <https://doi.org/10.1007/s12665-022-10676-3>.
- [46]. Pan, R., Wang, P., Zhou, Z., et al. (2023). Effects of confining stress on blast-induced damage distribution of rock with discontinuity. *Sustainability*. 15 (17): 13278.
- [47]. Siyu, P., Xibing, L., Jingyao G, et al. (2024). Energy evolution and failure mechanism of tunnel dynamic unloading in deep rock mass abounding in closable minor joints. *Tunnelling and Underground Space Technology*. 154: 163132.
- [48]. Cundall, P.A. (1971) A computer model for simulating progressive large scale movements in blocky system. Proc. *Rock Fracture: International Symposium on Rock Mechanics*. Nancy, France, 4-6 October 128-132.
- [49]. Jing, L. (2003). A review of techniques, advances and outstanding issues in numerical modelling for rock mechanics and rock engineering. *International Journal of Rock Mechanics and Mining Sciences*. 40 (3): 283–353.
- [50]. Zhu, J.B. (2013). DEM modeling of wave propagation through jointed rock mass. In: *Rock Dynamics and Applications: State of the Art*, Leiden, Netherlands: 443–49.
- [51]. Zhu, J.B., Deng, X.F., Zhao, X., et al. (2013). A numerical study on wave transmission across multiple intersecting joint sets in rock masses with UDEC. *Rock mechanics and rock engineering*. 46: 1429–1442.
- [52]. Ghaedi Ghalini, M., Bahaaddini, M. & Amiri Hossaini, M. (2022). Estimation of in-situ block size distribution in jointed rock masses using combined photogrammetry and discrete fracture network. *Journal of Mining and Environment*. 13 (1): 175–184.
- [53]. Rabiei-Vaziri, M., Tavakoli, H. & Bahaaddini M. (2022). Statistical analysis on the mechanical behaviour of non-persistent jointed rock masses using combined DEM and DFN. *Bulletin of Engineering Geology and the Environment*. 81 (5): 177.
- [54]. HajiMohammadi, M.A., Bahaaddini, M., Khosravi, M.H., et al. (2025). Assessment of discontinuities induced overbreak by tunnel advancement using discrete fracture network (Case study: Alborz Tunnel, Iran). *Journal of Mining and Environment*. <https://doi.org/10.22044/jme.2025.15465.2966>.
- [55]. Cundall, P.A. & Hart, R.D. (1992). Numerical modelling of discontinua. *Engineering computations*. 9 (2): 101–113.
- [56]. Karatela, E., Taheri, A., Xu, C., et al. (2016). Study on effect of in-situ stress ratio and discontinuities orientation on borehole stability in heavily fractured rocks using discrete element method. *Journal of Petroleum Science and Engineering*. 139: 94–103.
- [57]. Bahaaddini, M. & Rahimi M. (2018). Distinct element modelling of the mechanical behavior of intact rocks using Voronoi tessellation model. *International Journal of Mining and Geo-Engineering*. 52 (1): 61–68.
- [58]. Itasca Consulting Group. Inc. (2023). UDEC (Universal Distinct Element Code) user's manual. Minneapolis, Minnesota.
- [59]. Zhao, J. and Zhu, W. (2003). *Stability Analysis and Modelling of Underground Excavations in Fractured Rocks*, Elsevier.
- [60]. Hekmatnejad, A., Rojas, E., Saavedra, C., et al. (2022). Presentation of the universal discontinuity index (UDi) system and its application to predict the geometry of over-excavation along a tunnel at New El Teniente mine. *Engineering Geology*. 311: 106901.
- [61]. Dershowitz, W. & Einstein, H.H. (1988). Characterizing rock joint geometry with joint system models. *Rock mechanics and rock engineering*. 21: 21–51.
- [62]. Bhasin, R, and Høeg, K. (1998). Parametric study for a large cavern in jointed rock using a distinct element model (UDEC—BB). *International Journal of Rock Mechanics and Mining Sciences*. 35 (1): 17–29.



دانشگاه صنعتی شاهرود

نشریه مهندسی معدن و محیط زیست

نشانی نشریه: www.jme.shahroodut.ac.ir

انجمن مهندسی معدن ایران

تحلیل حساسیت محدوده خسارت حفاری تونل در توده سنگ های درزه دار

ماهان امیرخانی^۱، مجتبی بهاء الدینی^{۱*}، علی رضا کارگر^۱ و امین حکمت نژاد^۲

۱. دانشکده مهندسی معدن، دانشکده گان فنی، دانشگاه تهران، تهران، ایران

۲. گروه مهندسی معدن، دانشکده مهندسی، دانشگاه کاتولیک پاپی شیلی، سانتیاگو، شیلی

چکیده

پایداری تونل ها و حفاریات زیرزمینی در توده سنگ ها به طور قابل توجهی تحت تاثیر توسعه محدوده خسارت حفاری می باشد، که در آن ناپیوستگی ها، توزیع تنش و ناحیه گسترش شکستگی را تحت تاثیر قرار می دهند. در مطالعات قبلی انجام شده بر روی زون خسارت حفاری، توده سنگ غالباً به عنوان یک محیط پیوسته در نظر گرفته می شد، در حالی که وسعت زون خسارت حفاری می تواند تحت تاثیر سیستم درزه داری قرار گیرد. هدف این پژوهش، بررسی زون خسارت حفاری در اطراف یک تونل حفاری شده در توده سنگی درزه دار با استفاده از روش های شبکه شکستگی مجزا و المان مجزا می باشد. سه مدل شبکه شکستگی مجزا با شدت های درزه داری مختلف ۰/۵، ۱/۰ و ۱/۵ متر مربع بر متر مکعب ساخته شد تا مکانیسم های شکست پیشرونده و تکامل خسارت در اطراف تونل مورد بررسی قرار گیرد. سپس مدل های شبکه شکستگی مجزا به کد المان مجزا وارد شدند. مساحت ناحیه پلاستیک به عنوان معیاری برای میزان زون خسارت حفاری در نظر گرفته شد. تاثیر خواص مکانیکی درزه، شامل چسبندگی، زاویه اصطکاک، سختی نرمال و سختی برشی، مورد بررسی قرار گرفت. تحلیل حساسیت بدون بعد برای ارزیابی و مقایسه تاثیر هر پارامتر بر وسعت محدوده خسارت حفاری انجام شد. نتایج نشان می دهد که زاویه اصطکاک درزه، تاثیر گذارترین پارامتر در تمامی شدت های درزه داری می باشد. نتایج این پژوهش، درک دقیق تری از رفتار درزه و تاثیر آن بر پایداری تونل در شرایط زمین شناسی مختلف ارائه می نماید.

اطلاعات مقاله

تاریخ ارسال: ۲۰۲۵/۰۴/۰۷

تاریخ داوری: ۲۰۲۵/۰۵/۱۰

تاریخ پذیرش: ۲۰۲۵/۰۶/۰۲

DOI: 10.22044/jme.2025.16037.3091

کلمات کلیدی

زون خسارت
توده سنگ درزه دار
شبکه شکستگی مجزا
شدت درزه داری
روش المان مجزا